2016

Factorized Runge-Kutta-Chebyshev Methods

Stephen O'Sullivan
Dublin Institute of Technology, stephen.osullivan@dit.ie

FACTORIZED RUNGE–KUTTA–CHEBYSHEV METHODS

STEPHEN O'SULLIVAN

School of Mathematical Sciences, Dublin Institute of Technology, Kevin Street, Dublin 8, Ireland

ABSTRACT. The second-order extended stability Factorized Runge–Kutta–Chebyshev (**FRKC2**) class of explicit schemes for the integration of large systems of PDEs with diffusive terms is presented. **FRKC2** schemes are straightforward to implement through ordered sequences of forward Euler steps with complex stepsizes, and easily parallelised for large scale problems on distributed architectures. Preserving 7 digits for accuracy at 16 digit precision, the schemes are theoretically capable of maintaining internal stability at acceleration factors in excess of 6000 with respect to standard explicit Runge-Kutta methods. The stability domains have approximately the same extents as those of **RKC** schemes, and are a third longer than those of **RKL2** schemes. Extension of **FRKC** methods to fourth-order, by both complex splitting and Butcher composition techniques, is discussed.

A publicly available implementation of the **FRKC2** class of schemes may be obtained from `maths.dit.ie/frkc`

1. INTRODUCTION

Factorized Runge–Kutta–Chebyshev (FRKC) methods are well suited to the numerical integration of problems where diffusion limits the efficiency of standard explicit techniques. In general, such systems of PDEs may be presented as semi-discrete ordinary differential equations of the form

$$(1) \qquad\qquad w' = f(t,\, w).$$

Here, the associated Jacobian is assumed to have negative eigenvalues lying close to the real axis, a good approximation for many systems of interest in astrophysical contexts.

The main use of extended stability Runge–Kutta (ESRK) methods is to fill the gap between unconditionally stable but operationally complex implicit methods, and simply implemented explicit schemes which suffer from stability constraints for stiff problems. ESRK methods are particularly useful for problems involving diffusion, where the work required by standard explicit techniques goes as the inverse square of the mesh spacing, while for extended stability methods it goes as the inverse mesh spacing. ESRK explicit schemes may be broadly divided into factorized and recursive types.

Factorized ESRK methods are particularly straightforward to implement at second-order, consisting solely of forward Euler steps. At orders above two, splitting methods or, alternatively, additional finishing stages are required for nonlinear problems. First considered by [8, 9, 23], factorized ESRK methods fell out of common usage for some time, until revived in 1996 as SuperTimeStepping [4] at

---

E-mail address: `stephen.osullivan@dit.ie`.

first-order, and later extended to second-order applications in astrophysical simulations by means of Richardson extrapolation [21, 22]. DUMKA methods exist at third- and fourth-order [16].

The perennial problem with the factorized formalism has been that, when a very large number of stages is used, the internal amplification factors can easily drown numerical precision. Factorized methods have, as a result, largely taken a back seat to recursive methods which manage internal stability by mapping the three-term recurrence relations for orthogonal polynomials to the stability polynomials [25]. Recursive methods have been developed up to fourth-order [2, 3, 15, 17, 18, 24, 27].

In the following, a formulation of factorized methods is presented which has high internal stability, and is more straightforward to implement than recursive methods, and demonstrates comparable efficiency.

2. FRKC STABILITY POLYNOMIALS

Stability polynomials form the backbone of ESRK numerical schemes and encapsulate the linear stability properties. Linearising a system of semi-discrete ODEs

$$(2) \qquad\qquad\qquad w' = Aw,$$

the FRKC stability polynomial [20] is obtained by seeking a polynomial of degree L which yields a forward Euler scheme of order N for linear problems through its roots via

$$(3) \qquad W^L = W^0 + T\sum_{l=1}^{L} a_l f(W^{l-1}) \quad W^0 = w^n, \; w^{n+1} = W^L.$$

The M-th stability polynomial of order N, with $L = MN$, determined via $w^{n+1} = R_M^N(TA)w^n$, must match the first $N+1$ terms in the Taylor expansion of the evolution operator

$$(4) \qquad\qquad R_M^N(TA) = \mathrm{e}^{TA} + \mathcal{O}(TA)^{N+1}.$$

Equivalently, the linear order conditions may be expressed as constraints on the derivatives of the stability polynomial evaluated at zero:

$$(5) \qquad\qquad R_M^{N\,(n)}(0) = 1, \quad n = 1, \cdots, N.$$

In addition, stability requires that the polynomial is bounded according to

$$(6) \qquad\qquad |R_M^N(z)| \leq 1 \quad \forall \quad z = T\lambda.$$

The objective is to determine a closed form for the polynomial such that the extent of the stability domain along the negative real axis β is as great as possible.

It is shown in [20] that the FRKC stability polynomial of rank N, and degree L, is a sum of Chebyshev polynomials of the first kind given by

$$(7) \qquad\qquad B_M^N(z) = d_0^N + 2\sum_{k=1}^{N} d_k^N C_{kM}(z),$$

where C_{kM} is the Chebyshev polynomial of the first kind of degree kM, and the coefficients d_k are determined through the linear order conditions given by Equation 5. The resultant scheme follows immediately from the roots of the polynomial, ζ_l, with coefficients given by

$$(8) \qquad\qquad a_l = \frac{1}{M^2 \alpha_M} \; \frac{1}{1 - \zeta_l}.$$

The dependency of β on L is presented in Figure 1 at second-order ($N = 2$). While the optimal value for $\beta/L^2 \beta_{RK2}$ is 0.41 [26], where β_{RK2} is the conventional second order Runge–Kutta stability limit, values of 0.330, 0.333, and 0.25 are obtained for FRKC2, RKC [25], and RKL2 [18] respectively.
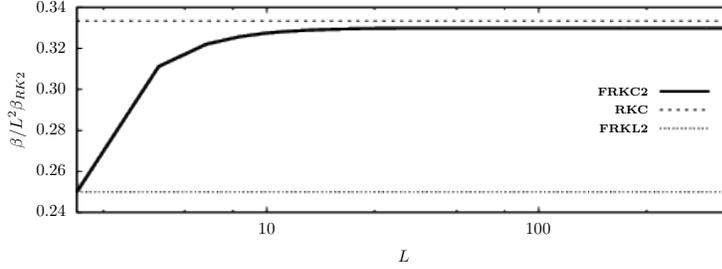
FIGURE 1. Extent of real stability domain at second-order for **FRKC2** (solid line). For large values of stage-number L, the scheme has a stability domain which is $0.33L^2$ times the extent of the reference second-order Runge–Kutta scheme. Also shown are the corresponding values for **RKC** (dashed line) and **RKL2** (dotted line).

2.1. **Damping.** Along the real axis on the interior of the stability domain of the stability polynomial, there are points which are marginally stable, as shown in Figure 2. This is remedied by introducing the damping parameter $\nu \equiv \nu_0/N$ via

$$(9) \qquad a_l = \frac{1}{(1-\nu)M^2\alpha_M} \frac{1-\mu_l}{1-(1-2\mu_l)\zeta_l},$$

and again enforcing the order conditions given by Equation 5 via Newton-Raphson iteration over the parameters μ_l, which consist of N distinct values, each repeated M times. As a result, the marginally stable maxima in $|R|$ along the real axis are scaled by $\sim (1-\nu_0)$ at the expense of reducing the extent of the stability domain β along the real axis by approximately $(1-\nu)$.

The damping process may also be used to make the scheme applicable to problems with small hyperbolic components, with Péclet numbers $Pe \lesssim 10$. For the case $Pe \approx 10$, illustrated in Figure 2, there is a 25% loss in the extent of the stability domain observed.
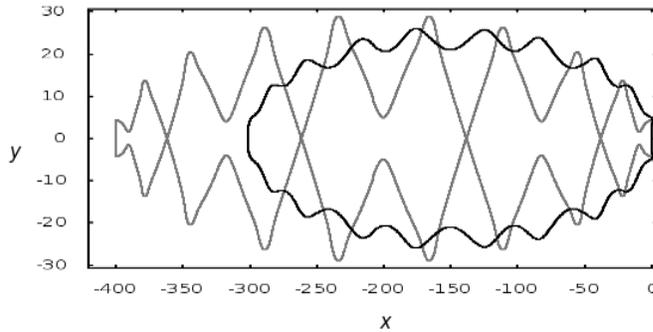

FIGURE 2. Stability domain $|R(x+Iy)| = 1$ for **FRKC** polynomial without damping (grey line) and with sufficient damping applied for mixed hyperbolic-parabolic problems with $Pe \approx 10$ (black line). The extent of the stability domain along the real axis is contracted by approximately 25% in the latter case.

2.2. **Internal stability.** Internal instability may be caused when the product of any of the possible sub-sequences of steps act to generate large values which drown out numerical precision. Following the idea of Lebedev [13, 14], but with a more effective approach, the timesteps are ordered to *approximately* minimise $\mathcal{Q}$, where

$$(10) \qquad \mathcal{Q} \equiv \max(\mathcal{Q}_{j,\,k}(x)), \quad 1 \leq j \leq k \leq L, \quad x \in [-\beta,\, 0],$$

is the maximum over the internal amplification factors defined by

$$(11) \qquad \mathcal{Q}_{j,\,k}(x) = \prod_{l=j}^{k} |1 + a_l x|.$$

While the optimal value of $\mathcal{Q}$ is approximately L^2, for the purposes of constructing a stabilization algorithm, a practical upper bound of $10L^2$ is chosen. In order to maintain this bound, the estimated maximum amplification factor $\overline{\mathcal{Q}}$ is held to a minimum while l runs from 1 to L, where

$$(12) \qquad \overline{\mathcal{Q}} \equiv \left\| \max \left(\prod_{j=1}^{l} v_{j,\,k}, \prod_{j=l+1}^{L/2} v_{j,\,k} \right) \right\|_1.$$

The amplification factors $v_{j,\,k}$ are defined by $v_{j,\,k} = |1 + a_j x_k|$, where $x_k \in [\overline{\beta},\, 0]$ are L uniformly distributed values over the reduced range $\overline{\beta} = (1 - nC)\beta$, with $C = 10^{-4}$. Initially, $n = 1$, however, in a limited number of cases, the process is repeated with n incremented until the required bound is satisfied. In this work, the mean value of n for the second-order schemes was found to be 1.5. Figure 3 shows the realised values of $\mathcal{Q}$ obtained via the stabilization algorithm for second-order schemes. Preserving 7 digits for accuracy, a scheme consisting of 10^4 stages is therefore theoretically viable in a numerical integration carried out to 16 digit precision.
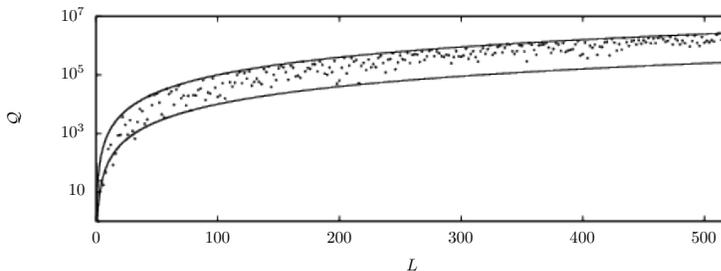

FIGURE 3. The maximum realised internal amplification factor $\mathcal{Q}$ as a function of L for second-order schemes. Guidelines are at L^2 and $10L^2$.

2.3. **Convex Monotone Property.** The convex monotone property (CMP) is of relevance to problems with spatially varying diffusion coefficients [18]. Figure 4 shows solutions obtained for a problem considered in [18] describing two materials placed into contact with differing temperatures and diffusion coefficients. For Chebyshev polynomial-based schemes such as **RKC** and **FRKC2**, noise in the solutions associated with failure to meet the CMP is evident if the schemes are forced to take steps with a uniform number of stages. Figures 4a and 4b illustrate this for the cases $L = 7$ and $L = 8$ respectively. The **RKL2** scheme maintains the CMP naturally with the result that the solution is smooth (Figure 4c). As shown in Figure 4d, for **FRKC2** with an identical number of function evaluations as used for

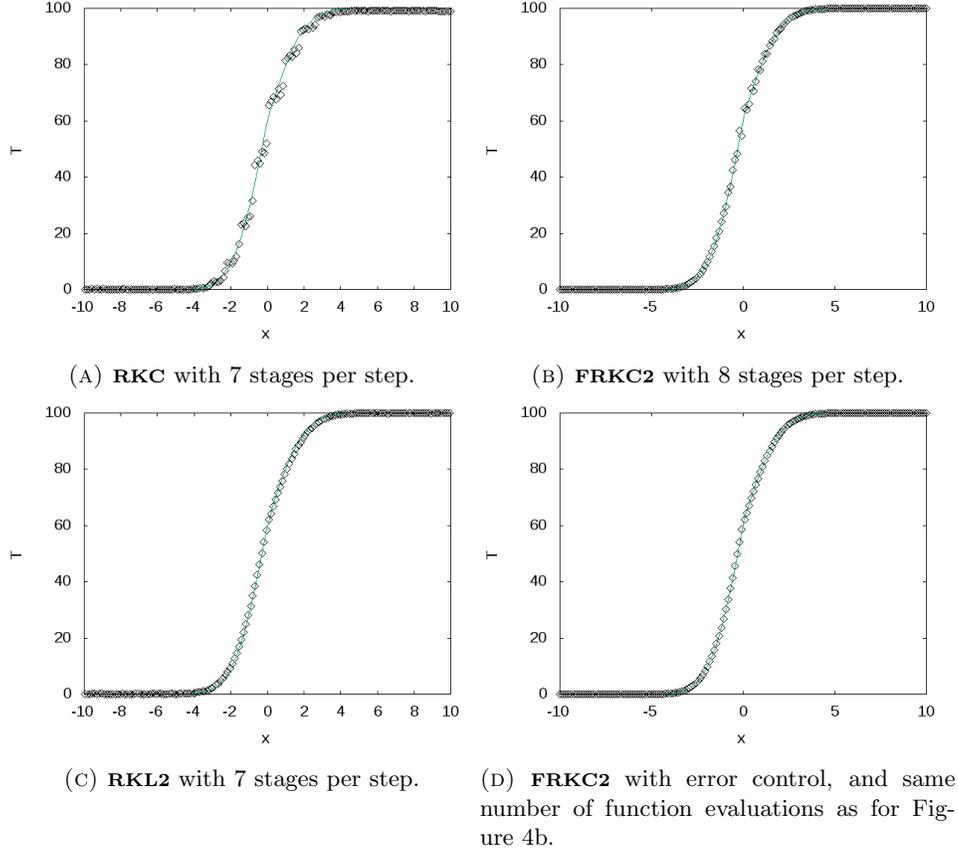Figure 4b, but with an error-control procedure (discussed further in Section 3), the noise is also absent.

(A) **RKC** with 7 stages per step.

(B) **FRKC2** with 8 stages per step.

(C) **RKL2** with 7 stages per step.

(D) **FRKC2** with error control, and same number of function evaluations as for Figure 4b.

FIGURE 4. Temperature across materials of different thermal conductivities illustrating the influence of the convex monotone property (CMP) [18].

3. **FRKC2** SCHEMES

A system $w' = f(w)$ is assumed such that the associated Jacobian has an eigenvalue of maximum magnitude $|\lambda|_{\max}$. Then, given a numerical solution w^n at some time index n, $L = 2M$ stages W^l (for $l = 0, \cdots, L$) are evaluated such that $W^0 = w^n$ and a second-order accurate solution $w^{n+1} = W^L$ is obtained a time T later. The intermediate stages of the scheme are determined via the Euler steps

$$(13) \qquad W^{l+1} = W^l + Ta_l f(W^l).$$

Error control is straightforward since a first-order solution is available at no additional cost in function evaluations. This first-order solution $\widehat{W}^L$ is obtained by considering only the real parts of a_l and $f(W^l)$. Setting $\widehat{W}^0 = W^0$,

$$(14) \qquad \widehat{W}^{l+1} = \widehat{W}^l + T \operatorname{Re}(a_l) \operatorname{Re}(f(W^l)).$$

The error, scaled to a specified tolerance TOL, is estimated using

$$(15) \qquad \|err\| = \left\| \frac{|W^{l+1} - \widehat{W}^{l+1}|}{TOL(1 + \max(|W^{l+1}|, |\widehat{W}^{l+1}|))} \right\|.$$

If $\|err\| > 1$, the step is rejected and retried with T scaled by $SAFE/\sqrt{\|err\|}$. Otherwise, a predictive controller is used to determine the subsequent timestep calibrated to the required tolerance via

$$(16) \qquad T^{n+1} = \left(\frac{SAFE}{\sqrt{\|err^n\|}} \right) \left(\frac{T^n}{T^{n-1}} \right) \sqrt{\frac{\|err^{n-1}\|}{\|err^n\|}},$$

using values of T and $\|err\|$ from previous timesteps. $SAFE$ is a safety factor chosen with a value 0.8 here. The reader is referred to [11] for further details of error control procedures.

3.1. **FRKC2 public code.** A freely available C implementation of the second-order **FRKC2** schemes may be accessed at `maths.dit.ie/frkc`. The files frkc2core.c and frkc2user.c provide the code for internal calculations required by the **FRKC2** scheme and the code specific to the particular problem respectively. For a given value of M, up to 257, the extent of the stability domain along the real axis, $\overline{\beta}$, and the maximum realised internal amplification factor $\mathcal{Q}$ (see also Figure 3) are given on line $3M - 2$ of frkc2arks.dat. The real and imaginary parts of a_l are recorded on lines $3M - 2$ and $3M$ respectively.
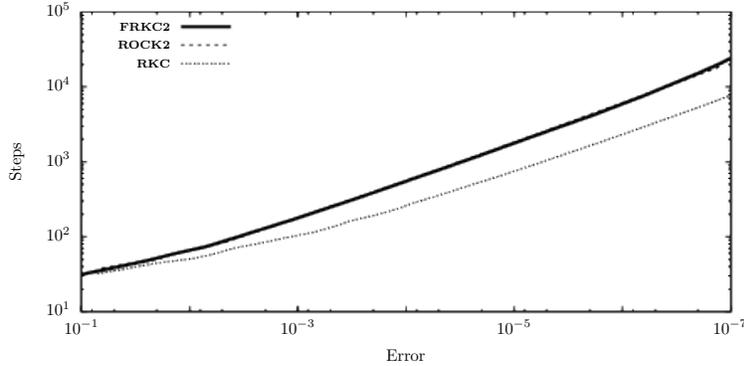

FIGURE 5. Efficiency comparison for the two-dimensional Brusselator problem for **FRKC2**, **ROCK2**, and **RKC**. (The lines for **FRKC2** and **ROCK2** are almost coincident.)

The default problem provided in frkc2user.c is a two-species reaction diffusion Brusselator

$$(17) \quad \begin{aligned} \partial v/\partial t &= 0.02 \left(\partial^2 v/\partial x_1{}^2 + \partial^2 v/\partial x_2{}^2 \right) + 1 - 4v + wv^2, \\ \partial w/\partial t &= 0.02 \left(\partial^2 w/\partial x_1{}^2 + \partial^2 w/\partial x_2{}^2 \right) + 3v - v^2 w, \\ v(0,\, x) &= 1 + \sin(2\pi x) \quad w(0,\, x) = 3 + \cos(2\pi y), \end{aligned}$$

which possesses a spectral radius of approximately 6400 for a 200×200 mesh. The initial state is a perturbation of the equilibrium solution [19] which is given by $v = 1$, $w = 3$. Figure 5 shows the number of steps required to attain a given error in the solution for **FRKC2**, **ROCK2** [1], and **RKC**. It is evident that, for a given precision, there is little difference in the number of steps required by **FRKC2** and **ROCK2**.

At higher degrees of acceleration (fewer steps), the difference between the three schemes is negligible.

4. FRKC4 SCHEME

4.1. **Complex splitting.** Above second-order, nonlinear order conditions are present which require additional consideration. One approach, given a semi-linear parabolic (reaction-diffusion) equation of the form $w' = Aw + f_B(w)$, is to split the nonlinear part $f_B(w)$, which is typically easily integrated, from the linear diffusion terms Aw. For orders above two, this requires complex timesteps [5,6] and may be prescribed in the form

$$(18) \qquad w^{n+1} = e^{T_{k_J} B} e^{T_{k_{J-1}} A} \cdots e^{T_{k_3} B} e^{T_{k_2} A} e^{T_{k_1} B} w^n.$$

Figure 6 shows the split FRKC4s scheme is competitive with ROCK4 [2]. However, in support of the splitting approach, it may be noted that ROCK4 suffers significantly from internal stability issues arising from the finishing stages required for the nonlinear order conditions (discussed further in Section 4.2) which effectively limits the scheme to about 150 stages.
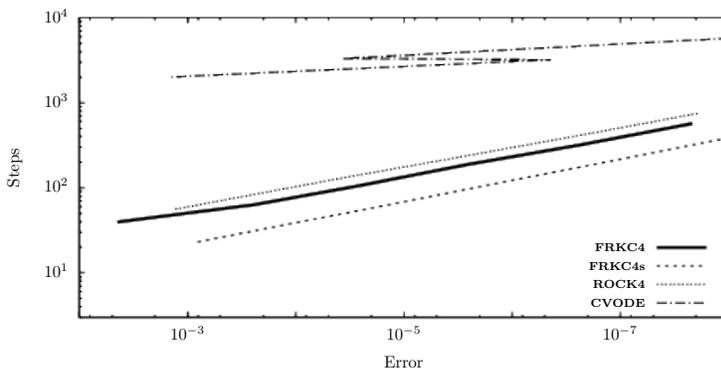

FIGURE 6. Performance results derived from the estimated error for the Brusselator problem. Shown are data for the fourth-order ESRK schemes FRKC4s, FRKC6s, ROCK4, and the fifth-order implicit CVODE scheme.

4.2. **Butcher composition.** An alternative to complex splitting is Butcher composition. At fourth-order, as illustrated in Table 1, $L - 4$ forward Euler steps are adopted from the FRKC stability polynomial with $N = 4$ as the scheme a, and appropriate finishing stages for the scheme $\bar{a}$ are subsequently derived.

0						
c_2	a_1					
c_3	a_1	a_2				
c_4	a_1	a_2	a_3			
$\vdots$	$\vdots$	$\vdots$	$\vdots$	$\ddots$		
c_L	a_1	a_2	a_3	$\cdots$	a_{L-5}	
	a_1	a_2	a_3	$\cdots$	a_{L-5}	a_{L-4}

0				
$\bar{c}_2$	$\bar{a}_{2\,1}$			
$\bar{c}_3$	$\bar{a}_{3\,1}$	$\bar{a}_{3\,2}$		
$\bar{c}_4$	$\bar{a}_{4\,1}$	$\bar{a}_{4\,2}$	$\bar{a}_{4\,3}$	
	$\bar{a}_1$	$\bar{a}_2$	$\bar{a}_3$	$\bar{a}_4$

TABLE 1. FRKC4 order composition tableaux.

According to a theorem of Hairer & Wanner [10], given the B-series a, b, the composite scheme ab is determined via

$$(19) \qquad a\overline{a}(t) = \frac{1}{\alpha(t)} \sum \left(\sum_{i=0}^{q} \binom{q}{i} \overline{a}(s_i(t)) \prod_{z \in d_i(t)} a(z) \right),$$

where rooted trees t are used to represent derivatives in Taylor series. The first summation in Equation 19 is over all $\alpha(t)$ different labelings of t, $s_i(t)$ is the subtree formed by the first i indices, and $\{z \in d_i(t)\}$ is the difference set of subtrees formed by the remaining indices. The eight order conditions at fourth order are then given by

$$
\begin{aligned}
(20) \quad
a\overline{a}(\bullet) &= a(\bullet) + \overline{a}(\bullet), \\
a\overline{a}(\tau_2) &= 2a(\bullet)\overline{a}(\bullet) + a(\tau_2) + \overline{a}(\tau_2), \\
a\overline{a}(\tau_3) &= 3a(\bullet)^2\overline{a}(\bullet) + 3a(\bullet)\overline{a}(\tau_2) + a(\tau_3) + \overline{a}(\tau_3), \\
a\overline{a}(\tau_3') &= 3a(\bullet)\overline{a}(\tau_2) + 3a(\tau_2)\overline{a}(\bullet) + a(\tau_3') + \overline{a}(\tau_3'), \\
a\overline{a}(\tau_4^{(1)}) &= 4a(\bullet)^3\overline{a}(\bullet) + 6a(\bullet)^2\overline{a}(\tau_2) + 4a(\bullet)\overline{a}(\tau_3) + a(\tau_4^{(1)}) + \overline{a}(\tau_4^{(1)}), \\
a\overline{a}(\tau_4^{(2)}) &= 4a(\bullet)^2\overline{a}(\tau_2) + 4a(\tau_2)a(\bullet)\overline{a}(\bullet) + (8/3)a(\bullet)\overline{a}(\tau_3) + (4/3)a(\bullet)\overline{a}(\tau_3') \\
&\quad + 2a(\tau_2)\overline{a}(\tau_2) + a(\tau_4^{(2)}) + \overline{a}(\tau_4^{(2)}), \\
a\overline{a}(\tau_4^{(3)}) &= 6a(\bullet)^2\overline{a}(\tau_2) + 4a(\bullet)\overline{a}(\tau_3') + 4a(\tau_3)\overline{a}(\bullet) + a(\tau_4^{(3)}) + \overline{a}(\tau_4^{(3)}), \\
a\overline{a}(\tau_4^{(4)}) &= 4a(\bullet)\overline{a}(\tau_3') + 6a(\tau_2)\overline{a}(\tau_2) + 4a(\tau_3')\overline{a}(\bullet) + a(\tau_4^{(4)}) + \overline{a}(\tau_4^{(4)}).
\end{aligned}
$$

Hence, for given scheme a, imposing the required order conditions on $a\overline{a}$ yields equations for $\overline{a}$, which are in turn easily solved for $\overline{a}$. The reader is referred to [10] for further details.

Figure 6 shows a comparison of the **FRKC4** scheme based on composition methods with other schemes. The reference solution is provided by a fifth-order implicit preconditioned BDF solver from the **CVODE** numerical package [7]. The number of steps required for a given precision is comparable for **ROCK4** and **FRKC4** and somewhat greater than the split **FRKC4s** scheme. This difference may be ascribed to a loss of precision due to the accumulation of errors over the finishing stages [12].

5. Conclusions

FRKC extended stability Runge–Kutta (ESRK) schemes are shown to well-suited to the integration of large-scale problems governed by systems of PDEs where the explicit timescale is constrained by diffusion. An implementation of the **FRKC2** second-order schemes, publicly available at `maths.dit.ie/frkc`, is presented. The fourth-order **FRKC4** schemes are also presented with nonlinear order conditions addressed via both splitting and composition methods. These schemes are shown to be competitive with alternative ESRK methods.

6. References

References

[1] Assyr Abdulle. *Chebyshev methods based on orthogonal polynomials*. PhD thesis, 2001.

[2] Assyr Abdulle. Fourth order Chebyshev methods with recurrence relation. *SIAM Journal on Scientific Computing*, 23(6):2041–2054, 2002.

[3] Assyr Abdulle and Alexei A Medovikov. Second order Chebyshev methods based on orthogonal polynomials. *Numerische Mathematik*, 90(1):1–18, 2001.

[4] V. Alexiades, G. Amiez, and P.A. Gremaud. Super-time-stepping acceleration of explicit schemes for parabolic problems. *Communications in numerical methods in engineering*, 12(1):31–42, 1996.

[5] Sergio Blanes, Fernando Casas, Philippe Chartier, and Ander Murua. Optimized high-order splitting methods for some classes of parabolic equations. *Mathematics of Computation*, 82(283):1559–1576, 2013.

[6] F. Castella, P. Chartier, S. Descombes, and G. Vilmart. Splitting methods with complex times for parabolic equations. *BIT Numerical Mathematics*, 49:487–508, 2009.

[7] Scott D Cohen and Alan C Hindmarsh. CVODE, a stiff/nonstiff ODE solver in C. *Computers in physics*, 10(2):138–143, 1996.

[8] W Gentzsch and A Schluter. On one-step methods with cyclic stepsize changes for solving parabolic differential equations. *Z. Angew. Math. Mech*, 58:T415–T416, 1978.

[9] A Guillou and B Lago. Domaine de stabilité associé aux formules dintégration numérique déquations différentielles, a pas séparés et a pas liés. recherche de formules a grand rayon de stabilité. *Ier Congr. Ass. Fran. Calcul., AFCAL*, pages 43–56, 1960.

[10] E. Hairer, S.P. Nørsett, and G. Wanner. Solving ordinary differential equations I: Nonstiff problems. *Springer series in computational mathematics*, 8, 1993.

[11] E. Hairer and G. Wanner. Solving ordinary differential equations II: Stiff and differential-algebraic problems. *Springer series in computational mathematics*, 14, 1996.

[12] Willem Hundsdorfer and Jan G Verwer. *Numerical solution of time-dependent advection-diffusion-reaction equations*, volume 33. Springer Science & Business Media, 2013.

[13] VI Lebedev. How to solve stiff systems of differential equations by explicit methods. *Numerical methods and applications*, pages 45–80, 1994.

[14] Vyacheslav Ivanovich Lebedev. Explicit difference schemes for solving stiff problems with a complex or separable spectrum. *Computational mathematics and mathematical physics*, 40(12):1729–1740, 2000.

[15] J Martin-Vaquero and B Janssen. Second-order stabilized explicit Runge-Kutta methods for stiff problems. *Computer Physics Communications*, 180(10):1802–1810, 2009.

[16] Alexei A Medovikov. High order explicit methods for parabolic equations. *BIT Numerical Mathematics*, 38(2):372–390, 1998.

[17] Chad D Meyer, Dinshaw S Balsara, and Tariq D Aslam. A second-order accurate Super TimeStepping formulation for anisotropic thermal conduction. *Monthly Notices of the Royal Astronomical Society*, 422(3):2102–2115, 2012.

[18] Chad D Meyer, Dinshaw S Balsara, and Tariq D Aslam. A stabilized Runge-Kutta-Legendre method for explicit super-time-stepping of parabolic and mixed equations. *Journal of Computational Physics*, 257:594–626, 2014.

[19] Gregoire Nicolis and Ilya Prigogine. *Self-organization in nonequilibrium systems : from dissipative structures to order through fluctuations*. Wiley, New York, 1977.

[20] Stephen O'Sullivan. A class of high-order Runge-Kutta-Chebyshev stability polynomials. *Journal of Computational Physics*, 300:665 – 678, 2015.

[21] Stephen O'Sullivan and Turlough P Downes. An explicit scheme for multifluid magnetohydrodynamics. *Monthly Notices of the Royal Astronomical Society*, 366(4):1329–1336, 2006.

[22] Stephen O'Sullivan and Turlough P Downes. A three-dimensional numerical method for modelling weakly ionized plasmas. *Monthly Notices of the Royal Astronomical Society*, 376(4):1648–1658, 2007.

[23] VK Saulev. Integration of parabolic equations by the grid method. *Fizmatgiz, Moscow*, 1960.

[24] BP Sommeijer, LF Shampine, and JG Verwer. RKC: an explicit solver for parabolic PDEs. *Journal of Computational and Applied Mathematics*, 88(2):315–326, 1998.

[25] P. J. van Der Houwen and B. P. Sommeijer. On the internal stability of explicit, m-stage Runge-Kutta methods for large m-values. *ZAMM - Journal of Applied Mathematics and Mechanics / Zeitschrift fr Angewandte Mathematik und Mechanik*, 60(10):479–485, 1980.

[26] Pieter Jacobus Van Der Houwen. *Construction of integration formulas for initial value problems*. North Holland, 1977.

[27] Jan G Verwer. Explicit Runge-Kutta methods for parabolic partial differential equations. *Applied Numerical Mathematics*, 22(1):359–379, 1996.